

Helicity and electron correlation effects on transport properties of double-walled carbon nanotubes

Shidong Wang and Milena Grifoni

Theoretische Physik, Universität Regensburg, 93040 Regensburg, Germany.

(Dated: May 12, 2017)

We analytically demonstrate helicity determined selection rules for intershell tunneling in double-walled nanotubes with commensurate (c-DWNTs) and incommensurate (i-DWNTs) shells. For i-DWNTs the coupling is negligible between lowest energy subbands, but it becomes important as the higher subbands become populated. In turn the elastic mean free path of i-DWNTs is reduced for increasing energy, with additional suppression at subband onsets. At low energies, a Luttinger liquid theory for DWNTs with metallic shells is derived. Interaction effects are more pronounced in i-DWNTs.

PACS numbers: 73.63.Fg, 71.10.Pm

Due to their unusual physical properties, cf. e.g. [1] carbon nanotubes have attracted lots of attention. Carbon nanotubes can be single-walled (SWNT) or multi-walled (MWNT), depending on whether they consist of a single or of several graphene sheets wrapped onto coaxial cylinders, respectively. Electronic properties of SWNTs are mostly understood [1]. In particular, SWNTs are usually ballistic conductors [2], and whether a SWNT is metallic or semiconducting is solely determined by its so called chiral indices (n, m) . Due to the one-dimensional character of the electronic bands at low energies, Luttinger liquid features at low energies have been predicted [3, 4] and observed [5, 6]. The situation however, is much less clear for MWNTs. Except for few experiments, see e.g. [7, 8], MWNTs are typically diffusive conductors, see e.g. [9, 10], with current being carried by the outermost shell at low bias [10, 11] and also by inner shells at high bias [12]. Intershell conductance measurements consistent with tunneling through orbitals of nearby shells have recently been reported [13]. Moreover, which kind of electron-electron correlation effects determine the observed zero-bias anomalies [14, 15] of MWNTs is still under debate. To better understand these features, i.e., the role of *intershell* coupling on transport properties of MWNTs, some experimental [16] and theoretical [17, 18, 19, 20, 21, 22, 23] works focussed on the simplest MWNT's realization, namely on double-walled nanotubes (DWNTs). One main outcome is that a relation must exist between the intershell coupling, shell helicity and transport properties. Specifically, two shell are called commensurate (incommensurate), if the ratio between their respective unit cell lengths along the tube axis, is rational (irrational) [1]. For example, using tight-binding models, Saito *et al.* [17] numerically found energy gaps opened by the intershell coupling in a DWNT with two armchair (and hence commensurate) shells. Ab-initio calculations [18, 19] confirmed these results. In general, numerical evidence of a negligible intershell coupling in DWNTs with incommensurate shells (i-DWNT) at low energies is found [17, 19, 20, 21].

In this Letter, we derive an analytical expression, yielding *helicity-dependent selection rules* for tunneling, for the effective intershell coupling. For i-DWNTs the intershell coupling is negligible between the *lowest* subbands but it becomes important when *higher* subbands are involved. We show that this in turn yields an elastic mean free-path which decreases with energy and which shows a characteristic suppression at subbands onset. Then by including intra- and inter-shell Coulomb interactions, we show that metallic DWNTs can be described by Luttinger liquid theory at low energies. The tunneling density of states has a power-law behavior with different exponents for i-DWNTs and commensurate-shells DWNTs (c-DWNTs).

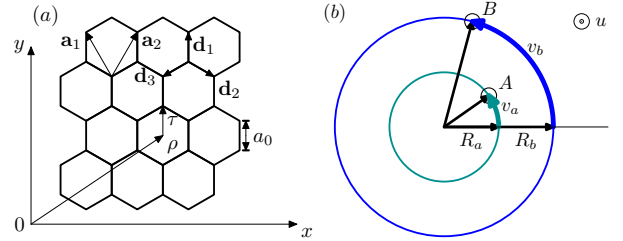


FIG. 1: (a) Graphene lattice. The x and y axes are along the armchair and zigzag axes respectively. The distance between two nearest carbon atoms is $a_0 \sim 1.42 \text{ \AA}$. The unit lattice vectors are \mathbf{a}_1 and \mathbf{a}_2 . The vectors \mathbf{d}_i connect three nearest neighbour atoms, while $\boldsymbol{\rho}$ and $\boldsymbol{\tau}$ are two vectors required to specify the position of a carbon atom. (b) Cross section of a DWNT. Atoms A and B in two shells of radii R_a and R_b , respectively, are projected onto this cross section.

To derive the helicity-dependent selection rules, we use a tight-binding model for non interacting electrons with one π -orbital per carbon atom [1] and follow [24]. This model is described by the Hamiltonian

$$H_0 = \sum_{\beta} \sum_{\langle ij \rangle} \gamma_0 c_{\beta i}^{\dagger} c_{\beta j} + \sum_{ij} t_{\mathbf{r}_{a_i}, \mathbf{r}_{b_j}} c_{a_i}^{\dagger} c_{b_j} + \text{H.c.}, \quad (1)$$

where $\beta = a, b$ is the shell index, $\langle ij \rangle$ is a sum over nearest neighbors in a shell, $\gamma_0 \sim 2.7 \text{ eV}$ [1] is the in-

trashell nearest neighbour coupling. The intershell coupling is $t_{\mathbf{r}_{ai}, \mathbf{r}_{bj}} = t_0 e^{-(d(\mathbf{r}_{ai}, \mathbf{r}_{bj}) - \Delta)/a_t}$, where $t_0 \sim 1.1$ eV, $\Delta \sim 0.34$ nm, $d(\mathbf{r}_{ai}, \mathbf{r}_{bj})$ is the distance between two atoms, and $a_t \sim 0.5$ Å [1]. We introduce the transformation

$$c_{\beta j} = \frac{1}{\sqrt{N_\beta}} \sum_{\mathbf{k}} e^{i\mathbf{k} \cdot \mathbf{r}_j} c_{\beta \eta(j)\mathbf{k}}, \quad (2)$$

where $\eta = \pm$ is the index for the two interpenetrating sublattices in a graphene sheet, and N_β is the number of graphene unit cells on a shell. The Hamiltonian reads

$$H_0 = \sum_{\beta \eta \mathbf{k}} \gamma_{\mathbf{k}} c_{\beta \eta \mathbf{k}}^\dagger c_{\beta - \eta \mathbf{k}} + \sum_{\mathbf{k}_a \mathbf{k}_b} \sum_{\eta_a \eta_b} \mathcal{T}_{\eta_a \eta_b}(\mathbf{k}_a, \mathbf{k}_b) c_{a \eta_a \mathbf{k}_a}^\dagger c_{b \eta_b \mathbf{k}_b} + \text{H.c.}, \quad (3)$$

where the *intrashell* coupling is $\gamma_{\mathbf{k}} = \sum_{j=1}^3 \gamma_0 e^{i\mathbf{k} \cdot \mathbf{d}_j} \equiv |\gamma_{\mathbf{k}}|s$, with \mathbf{d}_j the vectors connecting the three nearest neighbour carbon atoms. Introducing $\mathbf{r}_\beta = \mathbf{R} + \mathbf{X}_\beta$, with \mathbf{R} a lattice vector, $\mathbf{X}_\beta = \boldsymbol{\rho}_\beta + \eta_\beta \boldsymbol{\tau}$, where $\boldsymbol{\rho}_a - \boldsymbol{\rho}_b$ describes the relative position of the two shells, cf. Fig. 1, the elements of the *intershell* 2×2 coupling matrix are

$$\mathcal{T}_{\eta_a \eta_b}(\mathbf{k}_a, \mathbf{k}_b) = \sum_{\mathbf{G}_a \mathbf{G}_b} e^{i\mathbf{G}_a \cdot \mathbf{X}_a - i\mathbf{G}_b \cdot \mathbf{X}_b} t_{\mathbf{k}_a + \mathbf{G}_a, \mathbf{k}_b + \mathbf{G}_b}. \quad (4)$$

Here \mathbf{G} is the graphene reciprocal lattice vector

$$\mathbf{G} = \frac{4\pi}{3a_0} \left(\frac{\sqrt{3}}{2}(l_1 - l_2), \frac{1}{2}(l_1 + l_2) \right),$$

with $l_1, l_2 = 0, \pm 1, \pm 2, \dots$. Finally,

$$t_{\mathbf{q}_a, \mathbf{q}_b} = \frac{1}{A_{\text{cell}}^2 \sqrt{N_a N_b}} \int d\mathbf{r}_a d\mathbf{r}_b e^{i(\mathbf{q}_b \cdot \mathbf{r}_b - \mathbf{q}_a \cdot \mathbf{r}_a)} t_{\mathbf{r}_a, \mathbf{r}_b},$$

with A_{cell} the area of a graphene unit cell. We notice that the Hamiltonian Eq. (3) is diagonalized, in the absence of intershell coupling, by the transformation $U = \frac{1}{\sqrt{2}} \begin{pmatrix} s & s \\ -s & s \end{pmatrix}$. For later purposes, cf. Eq. (7), we call $\tilde{\mathcal{T}}_{\nu_a \nu_b} = (U^\dagger \mathcal{T} U)_{\nu_a \nu_b}$ the elements of the intershell tunneling matrix between two Bloch states in different shells. Here $\nu = \mp$ is the index for bonding/ antibonding states corresponding to negative/positive energies $\varepsilon_{\beta, \nu}(\mathbf{k})$ with $\beta = a, b$, respectively.

It is convenient to introduce coordinates u and v , which are along the tube axis and the circumference direction respectively, cf. Fig. 1(b). Then $\mathbf{k}_a \cdot \hat{\mathbf{v}} = k_{va}$ obeys $\ell_a = k_{va} R_a$, due to the periodic boundary conditions along the circumference. Likewise, $\ell_b = k_{vb} R_b$. Here, the integers ℓ_a and ℓ_b characterize energy subbands. In contrast, $k_u = \mathbf{k} \cdot \hat{\mathbf{u}}$ is continuous, cf. Fig. 2(b). The distance between two atoms $A = (R_a \cos(v_a/R_a), R_a \sin(v_a/R_a), u_a)$ and $B = (R_b \cos(v_b/R_b), R_b \sin(v_b/R_b), u_b)$ is then $d(\mathbf{r}_a, \mathbf{r}_b) \equiv D(v_a/R_a - v_b/R_b, u_a - u_b)$ where

$$D(z_1, z_2) = \sqrt{|R_a - R_b|^2 + 4R_a R_b \sin^2(z_1/2) + (z_2)^2}.$$

We then find $t_{\mathbf{q}_a, \mathbf{q}_b} = t \delta(q_{va} R_a - q_{vb} R_b) \delta(q_{ua} - q_{ub})$, where the prefactor t is calculated as

$$t = t_0 \int \frac{dz_1 dz_2 e^{-(D(z_1, z_2) - \Delta)/a_t}}{A_{\text{cell}}^2 \sqrt{N_a N_b}} \times e^{iz_1(q_{vb} R_b + q_{va} R_a)} e^{iz_2(q_{ub} + q_{ua})}.$$

Therefore, according to the two δ -functions in $t_{\mathbf{q}_a, \mathbf{q}_b}$, the effective intershell couplings $\mathcal{T}_{\eta_a \eta_b}(\mathbf{k}_a, \mathbf{k}_b)$ between two shells (n_a, m_a) and (n_b, m_b) are nonzero if they satisfy the following *selection rules*,

$$\ell_a + (n_a l_{1a} + m_a l_{2a}) = \ell_b + (n_b l_{1b} + m_b l_{2b}), \quad (5a)$$

$$k_{ua} + \mathcal{F}(n_a, m_a) = k_{ub} + \mathcal{F}(n_b, m_b), \quad (5b)$$

with $\mathcal{F}(n, m) = \frac{2\pi}{3a_0 \mathcal{L}(n, m)} ((n+2m)l_1 - (2n+m)l_2)$. Here $\sqrt{3}a_0 \mathcal{L}(n, m)$, with $\mathcal{L}(n, m) = \sqrt{n^2 + m^2 + nm}$, is the circumferential length of shell (n, m) . At low energies only the lowest subband determined by $3l_\beta = 2n_\beta + m_\beta$ in each shell is important, which *fixes* the values ℓ_a and ℓ_b . For c-DWNTs, e.g. if the two shells are either both arm-chair or zig-zag, Eqs. (5) can always be satisfied. Moreover, the dominant contribution is for $k_{ua} = k_{ub}$. On the other hand, for i-DWNTs, e.g. a (9,0)@(10,10), the selection rule Eq. (5b) can only be satisfied if the difference $k_{ua} - k_{ub}$ takes finite values. At low energies, this condition is never met. At higher energies higher subbands must be considered as well, and the selection rules can be satisfied. Notice that whenever the l.h.s. and r.h.s. of Eqs. (5) are not close to zero, the effective intershell coupling is exponentially suppressed [25]. We show now that, for i-DWNTs, the increase of the inter-shell tunneling is at the origin of an elastic mean-free path l_{el} which decreases with increasing energy, and which shows a characteristic suppression at each subband onset. Our analytical results are in agreement with recent ab-initio calculations, showing a cross-over from ballistic to diffusive behavior in DWNT as the energy increases [20, 21], as well as with the experimental observation that MWNT mostly exhibit diffusive behavior. To evaluate the elastic mean-free path $l_{el, b}(E) = v_F \tau_b(E)$ for electrons in the shell b , the life-time $\tau_b(E)$ for electrons with energy E is needed. Here $v_F = 8 \times 10^5$ m/s is the Fermi velocity for nanotubes. To be definite, $\hbar/\tau_b(E) = \sum_{\mathbf{k}, \nu = \pm} (\hbar/\tau_{b, \mathbf{k}\nu}) \delta(E - \varepsilon_{b, \nu}(\mathbf{k}))$, with $\varepsilon_{b, \nu}(\mathbf{k})$ the dispersion relation in shell b , and

$$\frac{\hbar}{\tau_{b, \mathbf{k}\nu}} = \sum_{\substack{\beta = a, b \\ \nu' = \pm}} \int dk'_u |T_{\mathbf{k}\mathbf{k}', \nu\nu'}^{b\beta}(\varepsilon_{b, \nu}(\mathbf{k}))|^2 \delta(\varepsilon_{b, \nu}(\mathbf{k}) - \varepsilon_{\beta, \nu'}(\mathbf{k}')). \quad (6)$$

For DWNTs the 4×4 T -matrix [28] is evaluated to be

$$T_{\mathbf{k}\mathbf{k}'}(\omega) = \mathcal{V}(\mathbf{k}, \mathbf{k}') + \sum_{\mathbf{k}_1} \mathcal{V}(\mathbf{k}, \mathbf{k}_1) G(\mathbf{k}_1, \omega) T_{\mathbf{k}_1 \mathbf{k}'}(\omega),$$

where $\mathcal{V}_{\nu_a \nu_b}^{ba}(\mathbf{k}, \mathbf{k}') = (\mathcal{V}_{\nu_a \nu_b}^{ab}(\mathbf{k}, \mathbf{k}'))^* = \tilde{\mathcal{T}}_{\nu_a \nu_b}(\mathbf{k}, \mathbf{k}')$ and $\mathcal{V}_{\nu\nu'}^{\beta\beta}(\mathbf{k}, \mathbf{k}') = 0$. The elements of the retarded

Green's function G are $G_{\nu\nu'}^{\beta\beta'}(\omega, \mathbf{k}) = (\omega - \varepsilon_{\beta,\nu}(\mathbf{k}) + i0^+)^{-1} \delta_{\beta\beta'} \delta_{\nu\nu'}$. For i-DWNTs $\tilde{T}_{\nu_a\nu_b}$ couples subbands with different energies, cf. Fig. 2. Thus, in general is $\varepsilon_{b,\nu}(\mathbf{k}) \neq \varepsilon_{a,\nu'}(\mathbf{k}')$, i.e., $\delta(\varepsilon_{b,\nu}(\mathbf{k}) - \varepsilon_{a,\nu'}(\mathbf{k}')) = 0$, and $\beta = b$ in Eq. (6). Hence, to lowest order in \tilde{T} , and if $\varepsilon_{b,\nu}(\mathbf{k}) \neq \varepsilon_{a,\nu'}(\mathbf{k}')$, the life-time $\tau_{b,\mathbf{k}\nu}$ is obtained inserting in Eq. (6)

$$T_{\mathbf{k}\mathbf{k}',\nu\nu'}^{bb}(\varepsilon_{b,\nu}(\mathbf{k})) = \sum_{\mathbf{k}_1,\nu_1=\pm} \frac{\tilde{T}_{\nu\nu_1}^*(\mathbf{k}, \mathbf{k}_1) \tilde{T}_{\nu_1\nu'}(\mathbf{k}_1, \mathbf{k}')}{\varepsilon_{b,\nu}(\mathbf{k}) - \varepsilon_{a,\nu_1}(\mathbf{k}_1) + i0^+}. \quad (7)$$

The elastic mean free paths $l_{el,(10,10)}$ and $l_{el,(9,0)}$ for electrons in the outer and inner shell, respectively, of a (9,0)@(10,10) DWNT are shown in Fig. 3. It is clearly shown that *before* the first subband onset, the motion is ballistic also for i-DWNTs of lengths up to $\simeq 5\mu m$.

In the remaining of the paper we consider only metallic shells and include electron-electron correlation effects in the low energy regime where only the first subband of each shell is populated. In this regime transport is ballistic for c-DWNTs as well as for i-DWNTs. Due to the linearity of the dispersion relation, a multi-channel Luttinger liquid description can be used [26, 27].

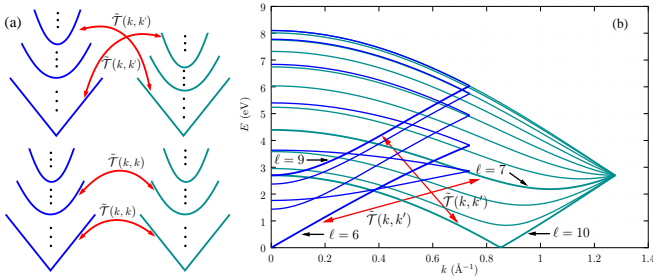


FIG. 2: (a) Schematics of the effect of the selection rules for i-DWNT (upper) and c-DWNT (down). (b) Energy subbands of the i-DWNT (9,0)@(10,10) in the absence of intershell coupling. The effect of the latter is to induce transitions between different subbands in different shells. The dominant coupling of the lowest armchair (zig-zag) subband is indicated.

At first, we consider an i-DWNT where the intershell coupling can be ignored. The unperturbed Hamiltonian can be written as

$$H_0 = -i\hbar v_F \sum_{r\alpha\sigma\beta} r \int du \psi_{r\alpha\sigma\beta}^\dagger \partial_u \psi_{r\alpha\sigma\beta}, \quad (8)$$

where $r = \pm$ is the index for right/left movers, $\alpha = \pm$ for the two independent Fermi points of a shell, and $\sigma = \pm$ for up and down spins. The electron density operator is $\rho_\beta(u) = \sum_{r\alpha\sigma\beta} \psi_{r\alpha\sigma\beta}^\dagger(u) \psi_{r\alpha\sigma\beta}(u)$. The two shells are only coupled by the Coulomb interaction, which gives rise to forward, backward, and Umklapp scattering processes. Experimentally, the Fermi points of nanotubes are usually shifted away from the half-filling due to doping or external gates. We assume that this is the case and

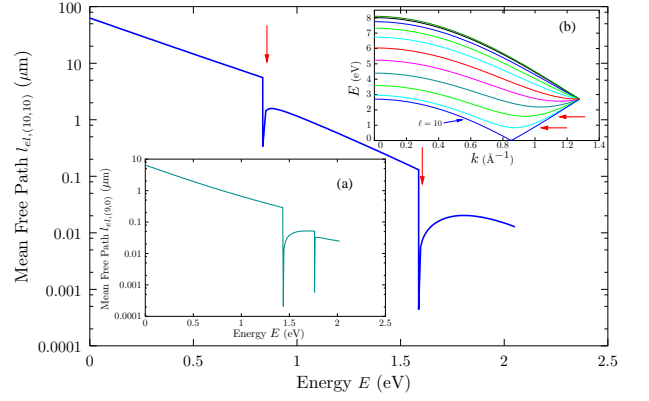


FIG. 3: Elastic mean free paths for electrons in the outer and inner (inset (a)) shells of the i-DWNT (9,0)@(10,10). Notice the dips in correspondence of the first two subband onsets.

hence neglect Umklapp processes. Since we are not interested in the extremely low temperature case, the backward scattering processes are also ignored here [26]. In the following, we only consider forward scattering processes described by the Hamiltonian

$$H_{\text{FS}} = \frac{1}{2} \sum_{\beta\beta'} \int dud' \rho_\beta(u) V_{\beta\beta'}(u-u') \rho_{\beta'}(u'), \quad (9)$$

with the effective one dimensional interaction

$$V_{\beta\beta'}(u-u') = \int_0^{2\pi R_\beta} \int_0^{2\pi R_{\beta'}} \frac{dvdv'}{(2\pi)^2 R_\beta R_{\beta'}} U_{\beta\beta'}(\mathbf{r}-\mathbf{r}'),$$

where $U(\mathbf{r})$ is the Coulomb interaction. The Hamiltonian $H = H_0 + H_{\text{FS}}$ can be diagonalized by the bosonization procedure discussed in Ref. [27]. We introduce bosonic field operators for the total/relative ($\delta = \pm$) charge/spin ($j = c, s$) modes in shell β , as well the total/relative ($\xi = \pm$) modes with respect to the two shells obeying the commutation relation $[\Theta_{j\delta\xi}(u), \phi_{j'\delta'\xi'}(u')] = -(i/2) \delta_{jj'} \delta_{\delta\delta'} \delta_{\xi\xi'} \text{sgn}(u-u')$. The Hamiltonian H can be then decoupled into 8 modes as

$$\sum_{j\delta\xi} \frac{\hbar v_{j\delta\xi}}{2} \int du \left(K_{j\delta\xi} (\partial_u \Theta_{j\delta\xi}(u))^2 + \frac{1}{K_{j\delta\xi}} (\partial_u \phi_{j\delta\xi}(u))^2 \right). \quad (10)$$

Only the two total charge modes are renormalized by the Coulomb interactions with velocities $v_{c\pm\pm} = v_F/K_{c\pm\pm}$ and interaction parameters

$$\frac{1}{K_{c\pm\pm}^2} = 1 + \frac{2}{\hbar\pi v_F} \left((\tilde{V}_{aa} + \tilde{V}_{bb}) \pm \sqrt{(\tilde{V}_{aa} - \tilde{V}_{bb})^2 + \tilde{V}_{ab}^2} \right), \quad (11)$$

where $\tilde{V}_{\beta\beta'} = \tilde{V}_{\beta\beta'}(2\pi/L)$ is the Fourier transform of the interaction potential at long-wave lengths, with L the nanotube length. The remaining modes are neutral with parameters $v_{j\delta\xi} = v_F$ and $K_{j\delta\xi} = 1$.

We consider now c-DWNTs where intershell tunneling is relevant. The intershell tunneling Hamiltonian is

$$H_t = \sum_{r\alpha\sigma} \tilde{T}_0 \int du \psi_{r\alpha\sigma a}^\dagger(u) \psi_{r\alpha\sigma b}(u) + \text{H.c.}, \quad (12)$$

where for simplicity the tunneling element $\tilde{T}_{++}(\mathbf{k}, \mathbf{k}')$ is evaluated at $\mathbf{k} = \mathbf{k}' = \mathbf{K}$ with the Fermi point \mathbf{K} of graphene, and is the constant \tilde{T}_0 . As detailed in [26], the Hamiltonian $H_0 + H_t$ can be exactly diagonalized. One finds the same form as in Eq. (8) where now the index $\beta = 0, \pi$ stands for bonding and antibonding states, respectively. Moreover, the Fermi wave vectors of the two independent Fermi points are shifted as $k_F^\alpha \rightarrow k_F^\alpha \pm (\tilde{T}_0/\hbar v_F)$ where \pm stand for π and 0 , respectively. We retain again only (intraband and interband) forward scattering described by the Hamiltonian Eq. (9), where now the scattering potentials $\tilde{V}_{\beta\beta'}$ are $\tilde{V}_{00} = \tilde{V}_{\pi\pi} = \tilde{V}_{0\pi}/2 = (\tilde{V}_{aa} + \tilde{V}_{bb} + \tilde{V}_{ab})/4$, so that bosonization brings again the total Hamiltonian in the form Eq. (11) with 6 neutral modes and 2 renormalized total charge modes. The tunneling density of states (TDOS) of both shells, $\rho_{b/a}(\varepsilon)$, immediately follows [29]. For i-DWNT is

$$\rho_{b/a}(\varepsilon) \sim |\varepsilon|^{\alpha_{b/a}},$$

with exponents $\alpha_{b/a}$ being different for electrons tunnelling into the middle or end of a nanotube:

$$\begin{aligned} \alpha_{\text{end},b/a} &= \frac{1}{4} \sum_{\xi=\pm} A_{b/a} \left(\frac{1}{K_{c+\xi}} - 1 \right), \\ \alpha_{\text{bulk},b/a} &= \frac{1}{8} \sum_{\xi=\pm} A_{b/a} \left(K_{c+\xi} + \frac{1}{K_{c+\xi}} - 2 \right). \end{aligned} \quad (13)$$

Here the coefficients $A_a, A_b = 1 - A_a$ are related to the eigenvalue problem [26, 27]. For c-DWNT is

$$\rho_{b/a}(\varepsilon) \sim |\varepsilon|^{\alpha_0} + |\varepsilon|^{\alpha_\pi} \Theta(\varepsilon - 2\tilde{T}_0),$$

where $\Theta(x)$ is the Heaviside step function and $2\tilde{T}_0$ is the gap between antibonding and bonding states. Because the intraband forward scattering potentials are equal, is $\alpha_0 = \alpha_\pi$. We find $\alpha_{\text{end/bulk}}$ given by Eq. (13) with $A_b = A_a = 1/2$. For illustration we calculate the tunneling exponents for the (10, 10) shell of a (9, 0)@(10, 10) and of a (5, 5)@(10, 10) with radii $R_a \approx 3.4 \text{ \AA}$ and $R_b \approx 6.8 \text{ \AA}$. We find $\alpha_{\text{end}} = 1.21, \alpha_{\text{bulk}} = 0.50$ for a (9, 0)@(10, 10) DWNT and $\alpha_{\text{end}} = 0.80, \alpha_{\text{bulk}} = 0.34$ for a (5, 5)@(10, 10) DWNT. For comparison, for a (10, 10) SWNT is $\alpha_{\text{end}} = 1.25$ and $\alpha_{\text{bulk}} = 0.52$. Hence, the exponents of DWNTs decrease due to the screening effect of the inner shell with respect to a SWNT. The intershell coupling reduces the exponents further. Notice that for Fermi liquids is $\alpha_{\text{end/bulk}} = 0$.

In summary, we derived selection rules according to which the intershell coupling is only negligible in i-DWNTs at low energies. An analytical expression in

Born-approximation for the elastic mean free path was provided. Including the Coulomb interaction, we developed a low energy Luttinger liquid theory for metallic DWNTs according to which the intershell coupling strongly reduces the tunneling density of state exponents in c-DWNT with respect to those of i-DWNTs.

The authors would like to thank G. Cuniberti, J. Keller and C. Strunk for useful discussions.

-
- [1] R. Saito, G. Dresselhaus, and M. S. Dresselhaus, *Physical Properties of Carbon Nanotubes* (Imperial College Press, London, 1998).
 - [2] C. T. White and T. N. Todorov, *Nature* **393**, 240 (1998).
 - [3] R. Egger and A. O. Gogolin, *Phys. Rev. Lett.* **79**, 5082 (1997); *Eur. Phys. J. B* **3**, 281 (1998).
 - [4] C. Kane, L. Balents, and M. P. A. Fisher, *Phys. Rev. Lett.* **79**, 5086 (1997).
 - [5] Z. Yao *et al.*, *Nature* **402**, 273 (1999).
 - [6] M. Bockrath *et al.*, *Nature* **397**, 598 (1999).
 - [7] S. Frank *et al.*, *Science* **280**, 1744 (1998).
 - [8] A. Urbina *et al.*, *Phys. Rev. Lett.* **90**, 106603 (2003).
 - [9] L. Langer *et al.*, *Phys. Rev. Lett.* **76**, 479 (1996).
 - [10] A. Bachtold *et al.*, *Nature* **397**, 673 (1999).
 - [11] A. Fujiwara, K. Tomiyama, and H. Suematsu, *Phys. Rev. B* **60**, 13492 (1999).
 - [12] P. G. Collins *et al.*, *Phys. Rev. Lett.* **86**, 3128 (2001)
 - [13] B. Bourlon *et al.*, *Phys. Rev. Lett.* **93**, 176806 (2004)
 - [14] A. Bachtold *et al.*, *Phys. Rev. Lett.* **87**, 166801 (2001).
 - [15] E. Graugnard *et al.*, *Phys. Rev. B* **64**, 125407 (2001).
 - [16] M. Kociak *et al.*, *Phys. Rev. Lett.* **89**, 155501 (2002).
 - [17] R. Saito, G. Dresselhaus, and M. S. Dresselhaus, *J. Appl. Phys.* **73**, 494 (1993).
 - [18] Y.-K. Kwon and D. Tomanek, *Phys. Rev. B* **58**, R16001 (1998).
 - [19] P. Lambin, V. Meunier, and A. Rubio, *Phys. Rev. B* **62**, 5129 (2000).
 - [20] F. Triozon *et al.*, *Phys. Rev. B* **69**, 121410(R) (2004).
 - [21] K.-H. Ahn *et al.*, *Phys. Rev. Lett.* **90**, 026601 (2003).
 - [22] S. Uryu, *Phys. Rev. B* **69**, 075402 (2004).
 - [23] J. Chen and L. Yang, *J. Phys. Cond. Matt.* **17**, 957 (2005).
 - [24] A. A. Maarouf, C. L. Kane, and E. J. Mele, *Phys. Rev. B* **61**, 11156 (2000).
 - [25] This holds, e.g. for finite length DWNTs, where conservation law for the wave vectors along the tube axis is broken but the selection law for the wave vectors along the circumference still holds.
 - [26] R. Egger, *Phys. Rev. Lett.* **83**, 5547 (1999).
 - [27] K. A. Matveev and L. I. Glazman, *Phys. Rev. Lett.* **70**, 990 (1993).
 - [28] G. D. Mahan, *Many-Particle Physics* (Plenum Press, 2000), 3rd ed.
 - [29] When contacts are deposited on the outer shell, and in STM experiments, the tunneling current through a DWNT probes the TDOS of the *outer* shell.